Electrically Tunable Nanoporous Carbon Hybrid Actuators

Li-Hua Shao, Juergen Biener, Hai-Jun Jin, Monika M. Biener, Theodore F. Baumann, and Jörg Weissmüller*

A novel nanoporous carbon/electrolyte hybrid material is reported for use in actuation. The nanoporous carbon matrix provides a 3D network that combines mechanical strength, light weight, and low cost with an extremely high surface area. In contrast to lower dimensional nanomaterials, the nanoporous carbon matrix can be prepared in the form of macroscopic monolithic samples that can be loaded in compression. The hybrid material is formed by infiltrating the free internal pore volume of the carbon with an electrolyte. Actuation is prompted by polarizing the internal interfaces via an applied electric bias. It is found that the strain amplitude is proportional to the Brunauer-Emmett-Teller (BET) mass specific surface area, with reversible volume strain amplitudes up to the exceptionally high value of 6.6%. The mass-specific strain energy density compares favorably to reported values for piezoceramics and for nanoporous metal actuators.

1. Introduction

Actuator materials change their dimensions upon converting electrical, thermal, chemical, or magnetic energy to mechanical energy. Technologically important examples are piezoelectric or electrostrictive ceramics and magnetostrictive materials.[1] As a rule, the implementation of these materials in devices requires sources of high voltage or magnetic field. Electrochemically driven actuator systems, by comparison, operate at much smaller and more readily implemented voltage values. This has sparked interest in these materials for applications ranging from microswitches to artificial muscles.[2–4] Considerable experimental and theoretical progress has been made in understanding the underlying charge-induced reversible strain effects in nanomaterials, and various actuator applications have been suggested for nanoporous noble metals,[4–7] carbon nanotubes (CNTs),[3,8–10] and graphene.[11,12] However, the applications of these materials are currently still limited by high materials costs and the fact that typical CNT and graphene arrays are poorly suited for loading in compression. It is therefore of interest to search for alternative low-cost actuator materials that combine the mechanical and chemical stability of carbon nanomaterials with the 3D architecture of nanoporous noble metals.

Nanoporous carbon foams have the potential to satisfy the above requirements: They can be inexpensive, mass-producible, and available as centimeter-sized mechanically robust monolithic materials that support compressive load. Reversible dimensional changes of porous carbon electrodes were first reported in 1972[13] and have later been confirmed on various carbon materials.[14–21] One point of interest in those studies is the mechanical behavior of supercapacitor devices. When ions are intercalated into the material at large and negative electrode potential, then large strain of up to 5% length change accompanies the charging/discharging cycles, and mechanical disintegration of the electrode may become an issue.[19]

The present study explores nanoporous carbon foams that are ideally suited for the actuator application (**Figure 1**). The skeletal structure of the material consists of interconnected, sub-micrometer sized particles that, after appropriate thermal activation, form networks in which essentially all carbon atoms are surface atoms (Figure 1c).[21] In this respect the material has similarities to CNTs and graphene, while its network structure qualifies it as a 3D solid. The resulting carbon structure is mechanically robust, even when its gravimetric surface area (up to 3200 m^2 g^{-1}) is comparable to that of a free-standing graphene sheet.

The systems investigated by us as electrochemically driven actuators are actually hybrid materials, in which the pore space of the nanoporous carbon matrix is filled with aqueous salt solutions or ionic liquids (Figure 1a). This type of nanocomposite structure, consisting of two phases with very different properties (e.g., solid versus liquid, electron conductive versus ion conductive), can exhibit novel functional properties that are not observed in the isolated phases. For example, reversible

L.-H. Shao, Prof. J. Weissmüller
Institut für Werkstoffphysik und Werkstofftechnologie
Technische Universität Hamburg-Harburg
Hamburg, Germany
E-mail: lihua.shao@tu-harburg.de
L.-H. Shao, Dr. H.-J. Jin
Institut für Nanotechnologie
Karlsruher Institut für Technologie
Karlsruhe, Germany
Dr. J. Biener, Dr. M. M. Biener, Dr. T. F. Baumann
Lawrence Livermore National Laboratory
Livermore, CA, USA
Prof. H.-J. Jin
Shenyang National Laboratory for Materials Science
Institute of Metal Research
Chinese Academy of Sciences
Shenyang, P. R. China
Prof. J. Weissmüller
Institut für Werkstoffforschung, Werkstoffmechanik
Helmholtz-Zentrum Geesthacht, Geesthacht, Germany

DOI: 10.1002/adfm.201200245

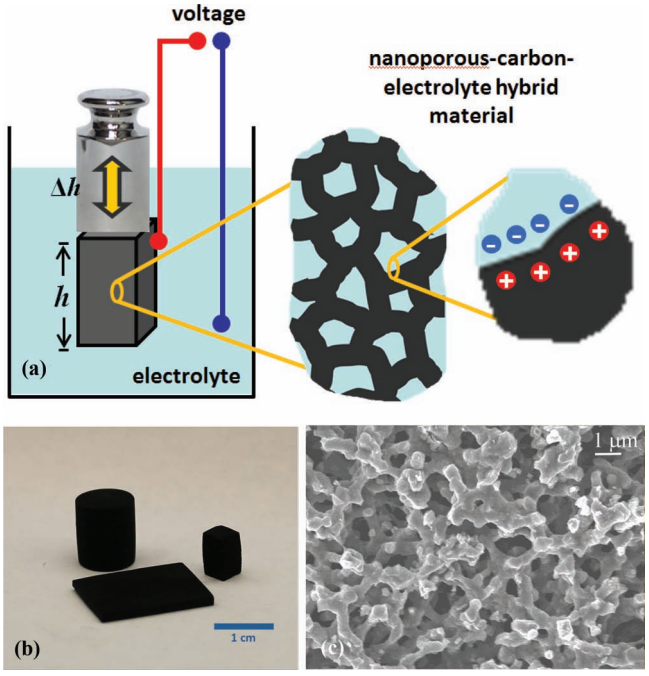

Figure 1. a) Schematic of the work principle of nanoporous-carbon-electrolyte hybrid material based actuator. b) Picture of nanoporous carbon samples. c) SEM image shows a 3D network architecture composed of micrometer-sized pores and ligaments.

electric control of the mechanical strength and flow stress has recently been discovered for a hybrid material of nanoporous metal containing perchloric acid.[22] Here, we show that the nanoporous-carbon-based hybrid material expands and contracts reversibly upon application of an electric bias between the two conduction channels, ionic and electronic. We report on the electrochemical-mechanical properties of this material and demonstrate that large volume strain values (up to 6.6%) and mass-specific energy densities can be realized. The strain amplitudes and strain energy densities exceed those of some conventional actuator materials. Thus, the material has potential for application as a low cost actuator.

2. Results and Discussion

We used nanoporous carbon samples with mass densities between 0.14 and 0.55 g cm^{-3} and with four different mass-specific BET (Brunauer-Emmett-Teller) surface areas, specifically 440, 1490, 2800, and 3032 m^2 g^{-1}.[21] Pore size distributions, as given in ref. [23], include smallest pores down to ≈1 nm in size. An aqueous solution of NaF (0.7 M) was chosen as the electrolyte. Fluoride anions are known to show little specific adsorption on carbon surfaces near the potential of zero charge (pzc).[24] This allows us to focus on capacitive double-layer charging with minimum contributions from chemisorption. The hybrid material is formed by infiltrating

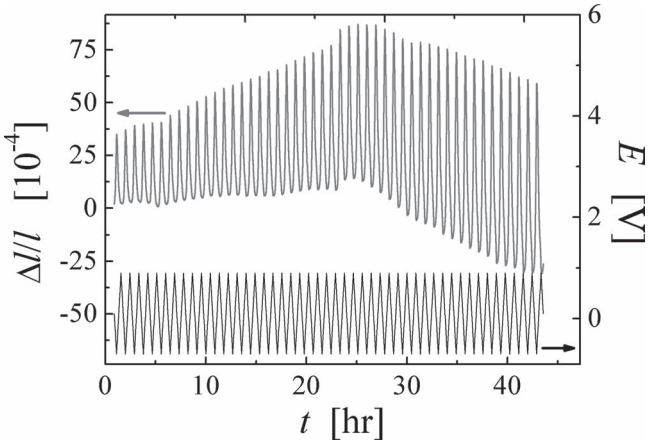

Figure 2. Relative length change, $\Delta l/l$, in response to the variation of the electrode potential, E, with time (t). Potential ranges from –0.7 to 0.9 V. Electrolyte is aqueous 0.7 M NaF, scan rate is 1 mV s^{-1}.

the free internal pore volume with the electrolyte. The imbibition is spontaneous, though with slow kinetics, as described below. The samples retain their structural integrity after wetting and even after repeated drying and re-wetting.

The conditioning of a fresh nanoporous carbon-hybrid sample during continuous cycling in 0.7 M NaF solution (–0.7 V to 0.9 V, 1 mV s^{-1}) is shown in **Figure 2**. The strain amplitude slowly increases with time for approximately one day and then stays constant. Similar to our previous work with porous carbon structures,[21] "fresh" samples of the present material tend to float upon their first contact with electrolyte, indicating that a major pore fraction is not immediately wetted. In agreement with that observation, the capacity as well as the strain amplitude in in situ dilatometry are initially small and increase during the first cycles. After repeated cycling both values stabilize, and the samples no longer float. This was taken as evidence for slow but spontaneous imbibition, implying that the electrolyte tends to wet the pore surfaces. In the example of Figure 2, the strain amplitude reached a value of nearly 1% in the final, wetted state.

Figure 3 compares charging current (Figure 3a) and the simultaneously recorded length changes (Figure 3b) for various scan rates. Expansion of the nanoporous-carbon hybrid

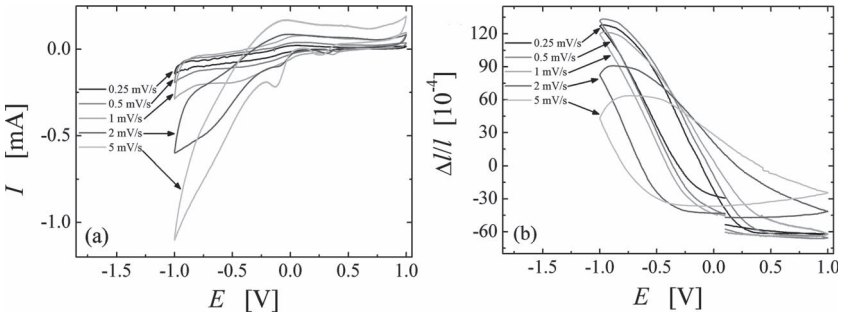

Figure 3. Simultaneously recorded data for electrochemical and mechanical behaviour of a nanoporous carbon hybrid actuator. Potential range is –1.0 to 1.0 V in 0.7 M NaF solution, results for different scan rates are shown. a) Cyclic voltammograms (current I vs. electrode potential E). b) Relative length change, $\Delta l/l$, vs. E.

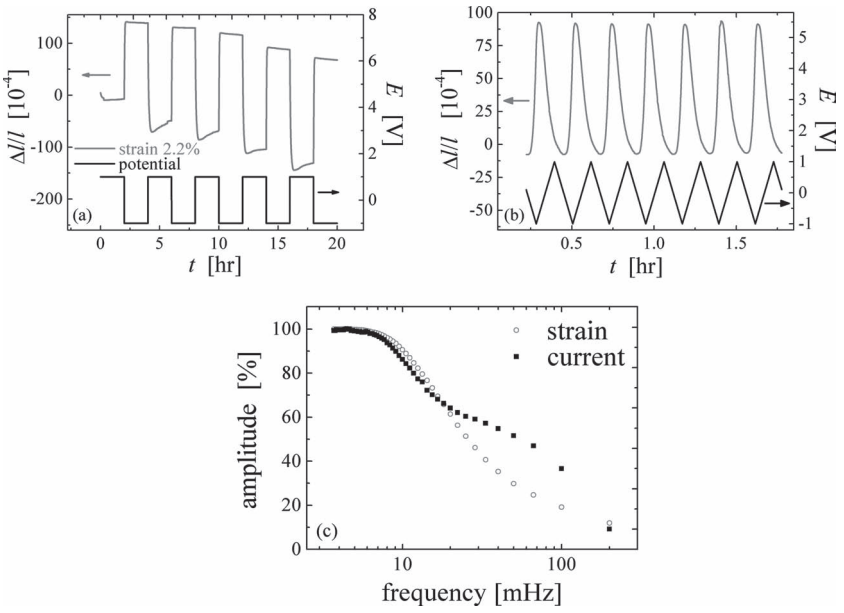

Figure 4. In situ dilatometry measurement of the nanoporous carbon hybrids with the potential range from –1.0 to 1.0 V in 0.7 M NaF solution. a) Strain $\Delta l/l$ in response to the potential E variation in the time (t) domain. b) Strain $\Delta l/l$ in response to the potential E variation at the scan rate of 5 mV s^{-1}. Note the strain changes reversiblely. c) Frequency dependence of the amplitude (% means that the percentage of the maximum strain amplitude) during potential jumps (rectangular wave). Squares: amplitude of the charging curve. Circles: amplitude of the length change as measured in the dilatometer.

material is observed for negative potentials (excess of electrons) and contraction is observed for positive potentials (depletion of electrons).

The charging rate experiments shown in Figure 3 reveal that the strain amplitude depends only weakly on the potential scan rate as long as that rate does not exceed 1 mV s^{-1}. This suggests that the experiment probes saturation strain values under these conditions. For higher scan rates, the strain amplitude decreases. The effect of scan rate on the actuator response is summarized in **Figure 4**. At low scan rates, very large strain amplitudes can be realized, but the strain amplitude slowly drifts thus indicating irreversible changes related to plastic deformation of the carbon matrix and/or to an electrochemical activation process (e.g., removing contamination at the surface of the sample) during the electrochemical scanning. By contrast, fully reversible strain cycles are achieved at higher scan rates (5 mV s^{-1}, Figure 4b).

At 2.2%, the uniaxial strain amplitude of Figure 4a is remarkable. It is noteworthy that the volume strain is even higher. By virtue of the synthesis, our material is statistically isotropic. Furthermore, the control parameter, namely the electrode potential, is a scalar, which does not impose directionality. For that reason, the strain in response to changes in the electrode potential must be isotropic. Therefore, the 2.2% linear strain translates into a volume strain of 6.6% (three times the length change). Both strain values considerably exceed what has been achieved with the same actuation scheme in nanoporous metals.[4,7] The strain amplitudes are also larger than those of the most common actuator material, namely piezoceramics, which typically exhibit strain amplitudes of 0.1–0.2%.[25] Even carbon nanotube arrays have only reached 1% strain in aqueous electrolyte.[3]

We note that the strain amplitude of 2.2% value is consistent with the 2% maximum variation in basal plane dimension that is observed for graphite intercalation compounds.[3] This may highlight the parallels between double-layer charging at the metal/electrolyte interface and charge transfer between intercalated atoms and the graphite basal planes of an intercalation compound. In fact, the observed response to charging, i.e., expansion (contraction) during electron injection (withdrawal), agrees well with the result of a density functional theory (DFT) study on charge-induced dimensional changes of graphite.[26] For CNTs the situation is more complex as the sign of the charge-induced strain depends on both chirality and diameter of the CNTs.[27,28] For example, Verissimo-Alves et al. found that the lattice constant of both metallic CNTs and graphene initially decreases, reaches a minimum, and then increases again with increasing hole accumulation. Semiconducting CNTs with small diameters ($d \leq 20$ Å), by contrast, always expand upon hole injection, and semiconducting CNTs with large diameters ($d \geq 20$ Å) display a behavior intermediate between those of metallic and large-gap CNT's.[27] More recently, Rogers and Liu reported a parabolic strain-potential relationship for monolayer graphene, and concluded that the electrostatic forces in the double layer dominate the actuation mechanism, as opposed to modified bond forces due to charge injection into the solid.[29] The varied points of view expressed in these studies highlight that the mechanism of charge-induced strain in carbon nanomaterials is poorly understood and requires further studies.

The characteristic time constants for charging (145 s) and strain response (165 s), were determined from potential jump experiments. Because of the limited sampling rate (10 s^{-1}) of the dilatometer, the time constant obtained from the charging curves is considered to be more accurate. Figure 4c shows the frequency dependence of the amplitude (in the form of percentage of the maximum strain amplitude) during potential jumps. The maximum strain amplitude can be achieved up to a repetition frequency of 7 mHz, consistent with the response time given above. This characteristic frequency, ω_c, decreases with decreasing electrolyte concentration and reaches 2 mHz for a 0.05 M NaF electrolyte solution. Much higher ω_c values (15 mHz) are observed for 1 M H_2SO_4 aqueous solution and 1-butyl-3-methylimidazolium tetrafluoroborate ($C_8H_{15}BF_4N_2$). For the actuator application, use of high conductivity electrolyte solutions is therefore preferable.[30,31]

Figure 5 presents the strain amplitudes of carbon-based hybrid samples with different mass specific surface areas, α_M (440, 1490, 2800, and 3030 m^2 g^{-1}) in the potential range from –0.7 V to 0.9 V (triangle) and –1.0 to 1.0 V (square), respectively. The plot shows a linear dependence of strain on the BET surface area, the slopes are 7.1×10^{-4} and 1.5×10^{-4} g m^{-2},

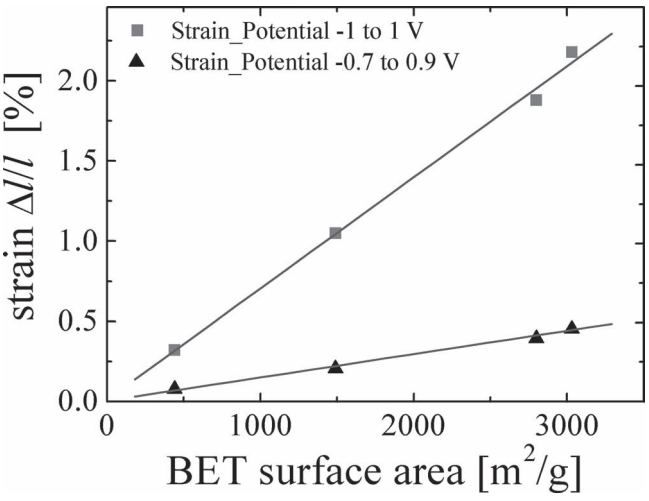

Figure 5. In situ scans with different nanoporous carbon-hybrid samples in 0.7 M NaF at the scan rate of 1 mV s^{-1} and in a potential range from −0.7 V to 0.9 V (triangles) and −1.0 to 1.0 V (squares), respectively.

respectively. The sample with the highest mass-specific surface area, i.e., 3030 m^2 g^{-1}, exhibits the largest strain. Our observation is consistent with what has been found for actuation in nanoporous metals.[4–7] The capillary forces at metal surfaces vary in proportion to the superficial charge density. Assuming a constant capacitance (capacity per area), a notion that is supported by experiments on the present material,[21] one expects a constant charge per area, independent of α_M, and thus a constant variation of the capillary force. For given variation of the capillary forces, the strain scales with the specific surface area per volume of solid. We thus expect a linear scaling between strain and α_M, in agreement with the observation.

Experiments on carbon electrodes for supercapacitor application have revealed even larger strain amplitudes, up to 5%, than those of the present work when cycled through large potential windows in organic electrolyte.[19] The strain accompanies intercalation, in other words, insertion of the ions in-between neighboring basal planes of the graphite. By contrast, the scaling between specific surface area and strain in our experiments would not be expected if species were inserted into the bulk, nor are the weakly adsorbing and strongly solvated Na^+ cations and F^- anions of our study likely candidates for intercalation. We therefore consider capacitive charging as the more likely scenario here. It is noted that electrochemically driven intercalation, or more generally the incorporation of substitutional atoms into bulk crystals, might be an alternative path to large strain actuation. Issues to be addressed in future studies in that field are the transport kinetics of the dissolved or intercalated species within the solid host phase and the possible mechanical disintegration of the material during repeated cycles. In the present work we maintain the focus on the capacitive processes in electrochemical actuation, which have been explored in more detail.

It is well known that in electrochemical actuator systems increasing the magnitude of the applied potential can increase the strain amplitude, which is also verified in this work. However, the method of increasing the potential to obtain larger strain values is limited by the onset of electrolysis of water that generates bubbles on the sample surface and decreases the lifetime of the actuator. For single-walled CNT actuators, strain values of 0.1–1% have been reported. Strain amplitudes of 0.15% have been reported for multiwalled CNT actuators even when potential windows as large as 4 V were used.[2] This is twice the potential window used in the present work. With the nanoporous-carbon hybrid material, the desired strain value can be adjusted by either adjusting the potential window, or by using the strain/BET surface area dependency shown in Figure 5.

An important parameter of an actuator is its work density, w. Assuming the actuator behaves like a linear elastic solid, the mass-specific strain energy density, w_M, is given as $w_M = \frac{1}{4} Y_{eff} \varepsilon^2_{max}/\rho$, where Y_{eff} is the effective macroscopic Young's modulus, ε_{max} is the maximum strain amplitude and ρ is mass density.[7] Actuator materials are commonly characterized in terms of an effective work density which is given as $\frac{1}{2} Y_{eff} \varepsilon^2_{max}/\rho$, twice the actual value.[7] In the interest of comparability with data by other authors we specify this higher value here.

The effective macroscopic Young's modulus Y_{eff} was measured in compression with a testing machine for miniature samples under controlled cross-head speed.[32] The displacement of the cross-head was recorded and empty runs produced a baseline used for correction the effects caused by the machine compliance. The engineering stress was determined as $\sigma = F/S_0$, where F is the force and S_0 is the initial area of sample cross section. The engineering strain ε is defined as $\delta l/l_0 \times 100\%$, where δl is the displacement of the sample upon compression and l_0 is the sample initial length. An example of a stress-strain curve obtained for a 3189 m^2 g^{-1} sample is shown in **Figure 6**. The strain range from 3% to 5% is used to calculate Y_{eff}, which emerges as 280 ± 2 MPa. Reported values of Y_{eff} for other monolithic, low-density carbon materials (such as carbon aerogels) cannot be quantitatively compared with the present ones since the density varies between materials, significantly affecting the stiffness.[33] Qualitatively, the reported values are similar[34,35] or larger[36,37] than the present one. We thus consider 280 MPa as

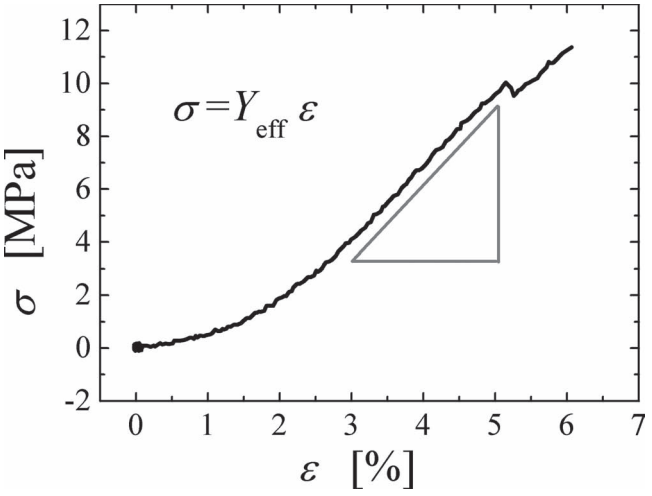

Figure 6. Stress–strain curve of nanoporous carbon-hybrid sample measured by a compression test.

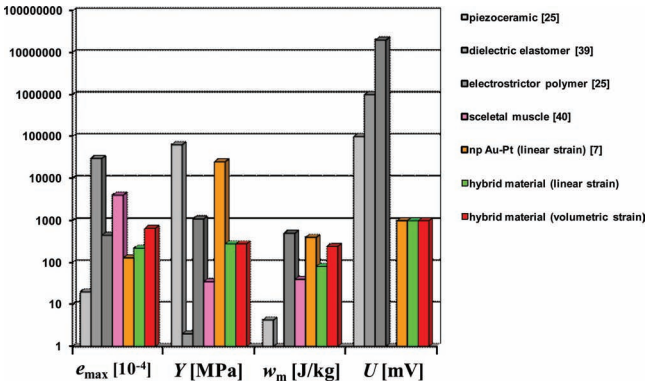

Figure 7. Column chart showing characteristics of various actuator materials. ε_{max}, maximum strain; *Y*, effective modulus; ω_m, mass-specific strain energy density; *U*, operating voltage for 100 µm actuator size.

a conservative value for the effective stiffness, that can be used to estimate the strain energy density. With this value, and using $\varepsilon_{max} = 2.2\%$, the result for $w_M = \frac{1}{2} Y_{eff} \varepsilon^2_{max}/\rho$ is 81 ± 3 J kg^{-1}.[38]

Selected figures of merit for different types of actuator materials are compared in **Figure 7**. The largest strain amplitudes are reached by dielectric elastomers[39] and by skeletal muscles,[40] and the highest stiffness is observed for piezoceramics[25] and nanoporous metals.[7] The nanoporous carbon hybrids show large strain amplitude and among the highest mass-specific strain energy densities. Importantly, and as compared to the conventional actuation materials shown in the chart, our hybrid materials are distinguished by their low operating voltage. A significant drawback of all electrochemically driven actuator systems, including the hybrid materials discussed here, is their slow response. Yet, for applications that tolerate actuation times in the order of seconds, nanoporous carbons are an attractive materials choice as they combine low voltage, large strain amplitude, high mass-specific strain energy density, and low material costs.

3. Conclusions

We have reported an electrically tunable nanoporous carbon hybrid actuator. The exceptionally large strain amplitude, high mass-specific strain energy, and the availability of centimeter-size monolithic samples distinguish the material as a candidate for use as a light-weight, low-cost actuator. The linear strain amplitude reaches 2.2% and, due to the isotropic materials structure, the volume strain is three times as high, i.e., 6.6%. Other nanoporous materials, such as Pt and Au, exhibit considerable lower values of the strain amplitude and strain energy densities. In fact, the mass-specific strain energy density of the hybrid material even exceeds that of piezoceramics.

4. Experimental Section

Sample Preparation: The nanoporous carbon material was synthesized through the acid-catalyzed sol-gel polymerization of resorcinol with formaldehyde to produce organic gels that are dried and subsequently pyrolyzed in an inert atmosphere. The details can be found in ref. [21]. As the working electrode, a cuboid nanoporous carbon sample (1 × 1 × 2 mm^3) was used. The same material was used as counter electrode but with an at least five times larger volume.

Electrochemical Measurements: The commercial dilatometer equipped with an in situ electrochemical cell was otherwise identical to that described in ref. [41]. Measurement procedures were analogous to ref. [21]. Ultrapure grade water (18.2 MΩ cm, Arium 611, Sartorius, Germany) plus NaF or H_2SO_4 (Suprapur, Merck), was used to prepare the electrolytes. All experiments were performed at room temperature, using commercial Ag/AgCl reference electrodes (+200 mV vs. a standard hydrogen electrode) in KCl solution (DRIREF-2, World Precision Instruments, Inc.).

Acknowledgements

Work at LLNL was performed under the auspices of the US DOE by LLNL under Contract DE-AC52-07NA27344. Project 12-ERD-035 was funded by the LDRD Program at LLNL.

Received: January 26, 2012
Revised: March 8, 2012
Published online: April 20, 2012

[1] S. A. Wilson, R. P. J. Jourdain, Q. Zhang, R. A. Dorey, C. R. Bowen, M. Willander, Q. Ul Wahab, M. Willander, S. M. Al-hilli, O. Nur, E. Quandt, C. Johansson, E. Pagounis, M. Kohl, J. Matovic, B. Samel, W. van der Wijngaart, E. W. H. Jager, D. Carlsson, Z. Djinovic, M. Wegener, C. Moldovan, R. Iosub, E. Abad, M. Wendlandt, C. Rusu, K. Persson, *Mater. Sci. Eng., R* **2007**, *56*, 1.
[2] Y. H. Yun, V. Shanov, Y. Tu, M. J. Schulz, S. Yarmolenko, S. Neralla, J. Sankar, S. Subramaniam, *Nano Lett.* **2006**, *6*, 689.
[3] R. H. Baughman, C. Cui, A. A. Zakhidov, Z. Iqbal, J. N. Barisci, G. M. Spinks, G. G. Wallace, A. Mazzoldi, D. De Rossi, A. G. Rinzler, O. Jaschinski, S. Roth, M. Kertesz, *Science* **1999**, *284*, 1340.
[4] J. Weissmüller, R. N. Viswanath, D. Kramer, R. Würschum, H. Gleiter, *Science* **2003**, *300*, 312.
[5] D. Kramer, R. N. Viswanath, J. Weissmüller, *Nano Lett.* **2004**, *4*, 793.
[6] J. Biener, A. Wittstock, L. A. Zepeda-Ruiz, M. M. Biener, V. Zielasek, D. Kramer, R. N. Viswanath, J. Weissmüller, M. Bäumer, A. V. Hamza, *Nat. Mater.* **2009**, *8*, 47.
[7] H.-J. Jin, X.-L. Wang, S. Parida, K. Wang, M. Seo, J. Weissmüller, *Nano Lett.* **2010**, *10*, 187.
[8] J. N. Barisci, G. M. Spinks, G. G. Wallace, J. D. Madden, R. H. Baughman, *Smart Mater. Struct.* **2003**, *12*, 549.
[9] R. H. Baughman, A. A. Zakhidov, W. A. de Heer, *Science* **2002**, *297*, 787.
[10] S. Liu, Y. Liu, H. Cebeci, R. Guzmán de Villoria, J.-H. Lin, B. L. Wardle, Q. M. Zhang, *Adv. Funct. Mater.* **2010**, *20*, 3266.
[11] J. Liang, Y. Huang, J. Oh, M. Kozlov, D. Sui, S. Fang, Ray H. Baughman, Y. Ma, Y. Chen, *Adv. Funct. Mater.* **2011**, *21*, 3778.
[12] X. Xie, L. Qu, C. Zhou, Y. Li, J. Zhu, H. Bai, G. Shi, L. Dai, *ACS Nano* **2010**, *4*, 6050.
[13] A. Soffer, M. Folman, *J. Electroanal. Chem.* **1972**, *38*, 25.
[14] Y. Oren, I. Glatt, A. Livnat, O. Kafri, A. Soffer, *J. Electroanal. Chem.* **1985**, *187*, 59.
[15] Y. Oren, A. Soffer, *J. Electroanal. Chem.* **1986**, *206*, 101.
[16] D. Golub, Y. Oren, A. Soffer, *J. Electroanal. Chem.* **1987**, *227*, 41.
[17] D. Golub, Y. Oren, A. Soffer, *Carbon* **1987**, *25*, 109.
[18] D. Golub, A. Soffer, Y. Oren, *J. Electroanal. Chem.* **1989**, *260*, 383.
[19] M. Hahn, O. Barbieri, R. Gallay, R. Kötz, *Carbon* **2006**, *44*, 2523.
[20] P. W. Ruch, R. Kötz, A. Wokaun, *Electrochim. Acta* **2009**, *54*, 4451.

[21] L.-H. Shao, J. Biener, D. Kramer, R. N. Viswanath, T. F. Baumann, A. V. Hamza, J. Weissmüller, *Phys. Chem. Chem. Phys.* **2010**, *12*, 7580.
[22] H.-J. Jin, J. Weissmüller, *Science* **2011**, *332*, 1179.
[23] J. Biener, M. Stadermann, M. Suss, M. A. Worsley, M. M. Biener, K. A. Rose, T. F. Baumann, *Energy Environ. Sci.* **2011**, *4*, 656.
[24] K. L. Yang, S. Yiacoumi, C. Tsouris, *J. Electroanal. Chem.* **2003**, *540*, 159.
[25] Q. Zhang, V. Bharti, X. Zhao, *Science* **1998**, *280*, 2101.
[26] G. Sun, M. Kertesz, J. Kürti, R. H. Baughman, *Phys. Rev. B* **2003**, *68*, 125411.
[27] M. Verissimo-Alves, B. Koiller, H. Chacham, R. B. Capaz, *Phys. Rev. B* **2003**, *67*, 161401(R).
[28] G. Sun, J. Kürti, M. Kertesz, R. H. Baughman, *J. Am. Chem. Soc.*, **2002**, *124*, 15076.
[29] G. W. Rogers, J. Z. Liu, *J. Am. Chem. Soc.* **2011**, *133*, 10858.
[30] *CRC Handbook of Chemistry and Physics* (Ed: D. R. Lide), Taylor and Francis Group, CRC press, Boca Raton, FL **2008**.
[31] Ionic Liquids Database-(IL Thermo), http://ilthermo.boulder.nist.gov/ILThermo/pureprp.uix.do?event = sort&source = pureindexilView133&value = Name, (accessed January 2012).
[32] O. B. Kulyasova, R. K. Islamgaliev, R. Z. Valiev, *Phys. Met. Metallogr.* **2005**, *100*, 83.
[33] M. A. Worsley, S. O. Kucheyev, J. H. Satcher Jr., A. V. Hamza, T. F. Baumann, *Appl. Phys. Lett.* **2009**, *94*, 073115.
[34] M. Krzesińska, A. Celzard, J. F. Marêché, S. Puricelli, *J. Mater. Res.* **2001**, *16*, 606.
[35] V. Palmre, E. Lust, A. Jänes, M. Koel, A.-L. Peikolainen, J. Torop, U. Johansona, A. Aabloo, *J. Mater. Chem.* **2011**, *21*, 2577.
[36] M. M. Brunoa, N. G. Cotellaa, M. C. Mirasa, T. Kochb, S. Seidlerb, C. Barbero, *Colloids Surf., A: Physicochem. Eng. Aspects* **2010**, *358*, 13.
[37] C. Balzer, W. Timo, S. Braxmeier, G. Reichenauer, J. P. Olivier, *Langmuir* **2011**, *27*, 2553.
[38] Our estimate of w_M is based on the mass density of the hybrid material (carbon plus electrolyte), 0.90 g cm^{-3}. For comparison with other electrochemical actuation schemes, we also specify the work density relative to the mass of carbon alone (0.14 g cm^{-3}) and ignoring the electrolyte. The value for w_M is then around six times higher, 490 J kg^{-1}.
[39] R. Pelrine, R. Kornbluh, Q. Pei, J. Joseph, *Science* **2000**, *287*, 836.
[40] J. D. W. Madden, B. Schmid, M. Hechinger, S. R. Lafontaine, P. G. A. Madden, F. S. Hover, R. Kimball, I. W. Hunter, *IEEE J. Oceanic Eng.* **2004**, *29*, 706.
[41] H.-J. Jin, S. Parida, D. Kramer, J. Weissmüller, *Surf. Sci.* **2008**, *602*, 3588.